A Method-of-Moments Model for Determination of Radiated Magnetic Field from Switch-Mode Power Supplies Components using Near-Field Measurement Data

S. M. M. Mirtalaei [1, 2], S. H. H. Sadeghi [1], and R. Moini [1]

[1] Department of Electrical Engineering
Amirkabir University of Technology, Tehran, 4413-15875, Iran
mirtalaei@aut.ac.ir, sadeghi@aut.ac.ir, moini@aut.ac.ir

[2] Department of Electrical Engineering
Islamic Azad University – Najafabad Branch, Najafabad, 8514143131, Iran

Abstract ─ Electromagnetic interference due to switching-mode power supplies (SMPSs) is a great concern for the designers of electrical and electronic equipment. In this paper, we propose a method-of-moments model for efficient determination of radiated magnetic field due to SMPSs mounted on printed circuit boards (PCBs). This model involves three stages. First, the magnetic field distribution on a given rectangular plan in the vicinity of the board is measured. The measured data are then used to identify the equivalent source currents on the surface of the radiating board by the method-of-moments. Having determined the radiating sources, the magnetic field distribution at a desired distance from the PCB can be computed. The main feature of the proposed model is its direct approach for reconstruction of the radiating current sources, which makes it much faster than the conventional techniques, involving heuristic optimization algorithms. The validity of the proposed technique is demonstrated by comparing the actual and predicted far-field magnetic field radiations due to a small electrical loop, a high frequency inductor as a typical radiating magnetic field component of SMPSs, and a microstrip transmission line, which simulating conduction paths on the PCB.

Index Terms ─ Electromagnetic compatibility, method-of-moments, near-field measurement, and switch-mode power supply.

I. INTRODUCTION

Switching mode power supplies (SMPSs) are commonly used in electronic and electric equipment as their input power source. The development of fast power semiconductor devices (MOSFET, IGBT, etc.) has increased the switching frequency of SMPSs, improving their power-volume ratio. However, the designers of SMPSs are greatly concerned about the resultant fast voltage and current variations, which can cause related elements to radiate, including PCB conduction paths, inductors, transformers, and heat sinks [1-7].

SMPSs have thus become important sources of electromagnetic interference (EMI). On the other hand, increasing integration of power electronic circuit modules together with the continuing growth in power density and switching frequency have resulted in a close interaction between SMPS components.

In order to design an SMPS system, which satisfies the requirements of electromagnetic compatibility (EMC) standards; designers typically use a set of established EMC rules to control various electromagnetic parameters [8]. SMPSs are commonly tested in a semi-anechoic chamber (SAC) or open area test site (OATS) to assess compatibility with EMC standards. If the EMC test fails, designers must modify their design and repeat the test. This process is very time-consuming and expensive, and thus, designers seek more efficient methods to predict radiated

Submitted On: Nov.13, 2012
Accepted On: June 23, 2013

emission form SMPSs and their related components in the early design stages. It is worth noting that SMPSs require high frequency inductors, transformers, and current loops, radiating strong magnetic and electric fields.

However, there is little work on the determination of radiated electric field form SMPSs [9] but determination of radiated magnetic field is more popular [10, 11]. Modeling approaches for determination of radiated magnetic field from SMPSs can be summarized in three categories. The first approach is based on a simplified analytical model for radiating components of SMPSs [1]. In this model, the transmission line theory is used for computing the electromagnetic field radiations in low frequency while a number of electrical dipoles are used for modeling the high frequency range radiations. These simplified analytical expressions are very crude approximations of radiated emission.

The second approach is based on the use of numerical methods. In [2], the system is simulated by a 3D finite element tool for modeling the governing equations, with source current or voltage extracted by measurement or standard circuit analysis. In [3], the finite-difference time-domain method is adopted to examine the electromagnetic resonant effects of various types of heat sinks, which are commonly used in SMPSs. Recommendations are proposed for optimal selection of heat sinks and the placement of components to mitigate potential EMC effects. Identification of source current and voltage and modeling all SMPS components in this approach is relatively complicated and cumbersome, making it unattractive for treating a complex SMPS. The third approach is based on the reconstruction of radiating sources on the respective PCB [4, 5]. This approach can be summarized in three distinct stages. First, the near-field data are measured. The measured data are then used to identify a set of equivalent radiating sources that generate the same field data as the original radiating sources. Finally, the field value at any point outside the board is computed by adding the contributions from all sources. Radiating sources in this method can be modeled as a current distribution on the PCB plane [4] or a set of electric and magnetic dipoles [5]. The determination of the equivalent radiating source from the near-field measured data in this method is based on the application of the electromagnetic equivalence principle [12], which involves optimization methods. Since the optimization process is time consuming, these methods are time-consuming and thus inappropriate for treating complex SMPSs [11].

In this paper, we adopt the source reconstruction approach described above for predicting radiated magnetic field from a typical SMPS and its related components. Here, we use the method-of-moments (MOM) to solve the governing integral equations, relating measured near magnetic fields with the equivalent surface electrical currents on the PCB plane. The proposed method offers several advantages. It is a direct method, and hence, is faster than those involve heuristic optimization techniques. Because of using analytic free-space Green's function, the stability of the computations in the proposed method is guaranteed and is not influenced by the sampling criteria for the fields [13].

The manuscript is organized as follows. In section II, the theory and basic formulation of the proposed method are presented. The validity of the proposed technique is demonstrated in section III where the actual and predicted far-field magnetic field radiations are compared, using simulation and experimental data.

II. THEORY

The geometry of the problem is shown in Fig. 1. As shown in this figure, a typical PCB is represented by radiating current sources located at z = 0. It is assumed that the PCB contains an SMPS together with related components, including several inductors, transformers, heat sinks, and PCB conduction paths among other electronic devices. The SMPS is operating at frequency f large enough to cause related components to radiate.

To determine the far-field ($z = h_2$ in Fig. 1) magnetic field distribution in the problem posed above, we adopt the electromagnetic equivalence principle [12]. According to this principle, a given set of sources (Fig. 2) bounded within a closed surface S can be characterized by equivalent electric currents (J) and magnetic currents (M) distributed on the surface S that encloses the original sources such that the generated fields outside the surface containing the sources are the same in both the original and the equivalent problem.

As a first step to determine the far-field radiations, we measure the tangential magnetic fields, H_x and H_y, on a rectangular plane ($z = h_1$ in Fig. 1) parallel to the plane of the PCB. The measurement plane, placed at a close vicinity of the PCB is assumed to be large enough to encompass all measurable values of magnetic field, resembling plane S in Fig. 2. It is worth noting that the number of measurement points is restricted by the probe structure and its sensitivity to field variations.

The measured magnetic field data are then used to identify the unknown equivalent current density ($\vec{J}_{eq} = J_{xeq}\hat{x} + J_{yeq}\hat{y}$) on the PCB plane ($z = 0$ in Fig. 1). This is done by ensuring that the measured data are the same as those obtained theoretically by the current sources.

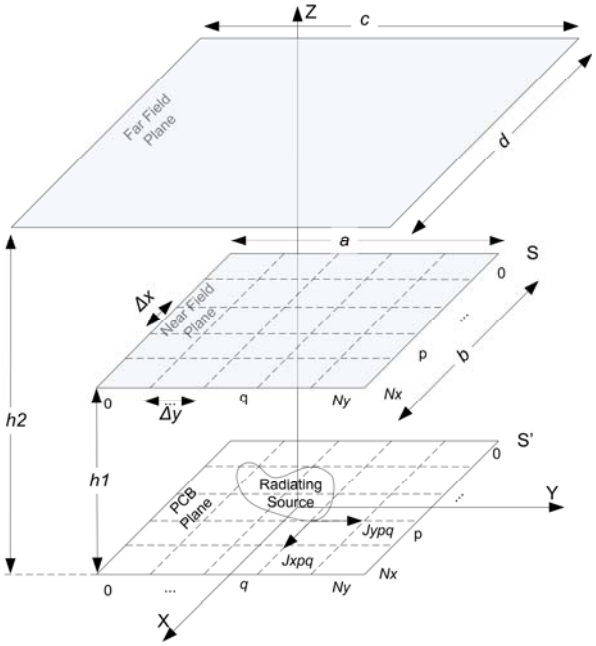

Fig. 1. Geometry of the problem, comprising the plane of radiating current sources at the location of PCB ($z = 0$), the measurement plane in the near filed zone ($z = h_1$) and the far-field plane ($z = h_2$) with unknown magnetic field distribution.

The magnetic field $\vec{H}$ in free space due to an arbitrary distribution of electric current J_{eq} is given as follows [14],

$$\vec{H} = \frac{1}{\mu_0}\nabla \times \vec{A}, \qquad (1)$$

where μ_0 is the permeability of free space and $\vec{A}$ is the auxiliary magnetic vector potential,

$$\vec{A} = \frac{\mu_0}{4\pi}\iint_{S'} \vec{J}_{eq}\frac{e^{-jkR}}{R}ds'. \qquad (2)$$

Here, R is the distance between source point (x',y',z') and observation point (x,y,z), k is the propagation constant and S' is the source surface.

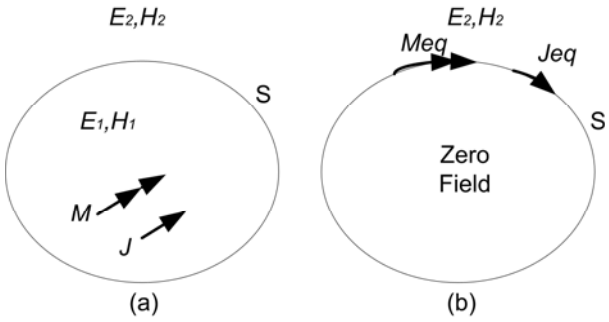

Fig. 2. The electromagnetic equivalence principle; (a) the original problem and (b) the equivalent problem.

By expanding equations (1) and (2) in the Cartesian coordinates, the values of the tangential magnetic field on the near-field plane, H_x and H_y, can be determined as follow,

$$H_x = \frac{1}{4\pi}\iint_{S'}[(z)J_y]\frac{1+jkR}{R^3}e^{-jkR}dx'dy' \qquad (3)$$

$$H_y = \frac{1}{4\pi}\iint_{S'}-[(z)J_x]\frac{1+jkR}{R^3}e^{-jkR}dx'dy', \qquad (4)$$

where J_x and J_y represent, respectively, the x- and y- components of the unknown equivalent current density (J_{eq}) on the PCB plane, S'.

To determine J_x and J_y in equations (3) and (4), we use the method-of-moments [15]. This is done by expanding $\vec{J}_{eq}$ in terms of the appropriate basis functions in sub-domains formed by discrediting S' in N_x and N_y segments along the x- and y-axes, respectively. The use of pulse basis function with constant amplitude and phase, we have,

$$\vec{J}_{eq} = \sum_{p=1}^{N_x}\sum_{q=1}^{N_y}(J_{pqx}\hat{x} + J_{pqy}\hat{y})\Pi(x - x_p, y - y_q) \qquad (5)$$

where

$$\Pi(x,y)=\begin{cases}1 & |x|<\dfrac{\Delta x}{2},|y|<\dfrac{\Delta y}{2}\\ 0 & |x|>\dfrac{\Delta x}{2},|y|>\dfrac{\Delta y}{2}\end{cases}, \quad (6)$$

$$x_p = p\Delta x - \frac{\Delta x}{2}, \quad (7)$$

$$y_q = q\Delta y - \frac{\Delta y}{2}, \quad (8)$$

and J_{pqx} and J_{pqy} are, respectively, the unknown coefficients associated with the *x*- and *y*-components of $\vec{J}_{\text{eq}}$ on sub-domain pq.

Substituting equation (5) into equations (3) and (4), the integral equations relating the magnetic fields to their equivalent electrical currents lead to a system of linear equations where the number of equations is equal to the number of measurement points, i.e.,

$$H_x = \sum_{i=0}^{N_x}\sum_{j=0}^{N_y}\frac{1}{4\pi}[(z)\,J_{yij}]\frac{1+jkR_{ij}}{R_{ij}^{\,3}}e^{-jkR_{ij}}\Delta x\Delta y, \quad (9)$$

$$H_y = \sum_{i=0}^{N_x}\sum_{j=0}^{N_y}\frac{1}{4\pi}[(-z)J_{xij}]\frac{1+jkR_{ij}}{R_{ij}^{\,3}}e^{-jkR_{ij}}\Delta x\,\Delta y, \quad (10)$$

or, in matrix form,

$$[H_x]=\left[Z_{H_x,J_y}\right][J_y], \quad (11)$$

$$[H_y]=\left[Z_{H_y,J_x}\right][J_x], \quad (12)$$

where

$$Z_{H_x,J_y}(i,j)=\frac{1}{4\pi}(z)\frac{1+jkR_{ij}}{R_{ij}^{\,3}}e^{-jkR_{ij}}\Delta x\,\Delta y, \quad (13)$$

$$Z_{H_y,J_x}(i,j)=-\frac{1}{4\pi}(z)\frac{1+jkR_{ij}}{R_{ij}^{\,3}}e^{-jkR_{ij}}\Delta x\Delta y. \quad (14)$$

Since Z_{H_x,J_y} and Z_{H_y,J_x} are large and sparse, the factorization methods are generally not efficient for solving equations (11) and (12). Instead, we use an iterative method such as the least square residual (LSQR) method to treat the problem in [16]. Having determined the unknown current sources on the PCB, the radiated far-field magnetic field can be readily obtained, using equations (3) and (4).

III. MODEL VERIFICATION AND RESULTS

To demonstrate the validity of the solution technique, we first consider the special case of a small electrical loop for which the results are available in the literature. We then present the theoretical and experimental results for a high frequency inductor, which is a typical component of an SMPS, radiating strong magnetic field and a microstrip transmission line, which simulating conduction paths on the PCB.

The setup shown in Fig. 3 is used to prepare the experimental results supporting the theoretical modeling. The setup consists of a Rohde & Schwarz Hz-11 EMI probe set, a three-dimensional motorized computer controlled scanner, and a Rohde & Schwarz ZVK-4GHz vector network analyzer. The probe is an H-field loop probe with 10 mm diameter [17].

A. Small electrical loop

In order to demonstrate the robustness of the model, simulated results are presented. In these simulations, the source is a small electrical loop of radius r = 10 mm placed at the location of the PCB (h = 0 in Fig. 1) as a radiating source. The loop is excited with a 1A sinusoidal current source of frequency 30 MHz. Figure 4 shows variations of the tangential magnetic field (H_x and H_y) produced by the small electrical loop on the near-field plane (h_1 = 10 mm, a = 100 mm, and b = 100 mm in Fig. 1.) [8]. To show the effect of the measurement noise on the simulated data, the values of H_x and H_y on the near-field plane are superposed by Gaussian noise with various signal-to-noise ratios (SNRs). The noisy data are then used as input measurement entries to the proposed model, producing equivalent electrical current distribution on the PCB. The equivalent current distribution is then used to compute the field distribution on the far-field plane (h_2 = 50 mm, c = 400 mm and d = 400 mm). A comparison of the actual and reconstructed results for the SNR = 30 dB shown in Figs. 6 (a) and (b), respectively, demonstrates the validity of the proposed model. The results indicate that the model is capable of accurately reconstructing magnetic field distributions at far-field regions. A quantitative comparison of these results can also be found in Table I where the mean-square deviation, *MSD*, between the actual tangential magnetic field

$H_{tn}(n=1,2,...,N)=\sqrt{H_{xn}{}^2+H_{yn}{}^2}$, and its reconstructed counterpart, $\hat{H}_{tn}(n=1,2,...,N)$ in all cases are given by,

$$MSD=\frac{\sum_{n=1}^{N}\left(H_n-\hat{H}_n\right)^2}{\sum_{n=1}^{N}H_n^2}. \qquad (15)$$

To study the effect of sampling distance (Δx and Δy in Fig. 1) on the accuracy of the proposed technique, we have used several simulated field data on the measurement plane (i.e., $z = h_1$ in Fig. 1) with various degrees of coarseness. A quantitative comparison between the actual and reconstructed field distributions on the far-field plane (h_2 = 50 mm, c = 400 mm, and d = 400 mm) can be found in Table II. From the results illustrated in this table, it is revealed that the proposed technique is readily converged for a wide range of sampling distances on the field measurement plane. However, the number of measurement data should be large enough to achieve accurate results.

Fig. 3. Experimental setup for magnetic field measurements.

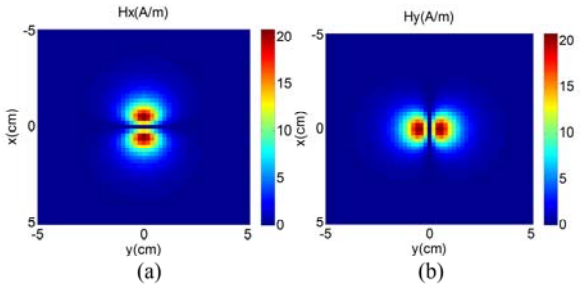

Fig. 4. Variations of the tangential magnetic field produced by the electrical loop on the near-field plane (h_1 =10 mm); (a) H_x and (b) H_y.

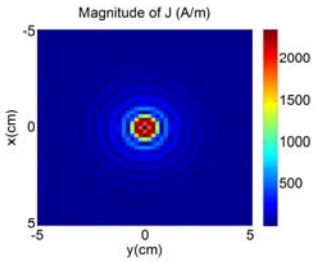

Fig. 5. Variations of the equivalent current ($|J|$) on the PCB plane (h = 0) predicted by the proposed model, using the data shown in Fig. 4.

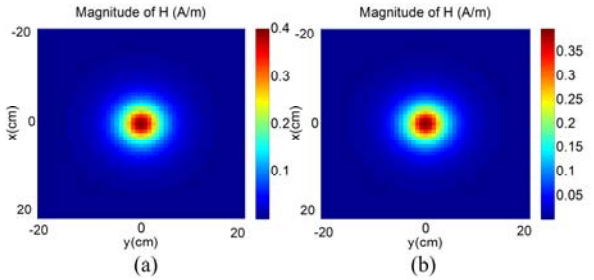

Fig. 6. Variations of the tangential magnetic field ($\sqrt{H_x^2+H_y^2}$) produced by the electrical loop on the far-field plane (h_2 = 50 mm); (a) theoretical and (b) reconstructed results.

Table I: Values of the MSD for several SNRs.

	SNR=30dB	**SNR=20dB**	**SNR=10dB**
MSD	0.0451	0.1698	0.4992

Table II: Values of the MSD and computation time for various sampling distances on the field measurement plane.

Δx =Δy	**2mm**	**5mm**	**10mm**	**20mm**
MSD	0.04	0.15	0.22	0.63
Time (sec)	279.24	1.78	0.281	0.16

B. High frequency inductor

To further examine the validity of the proposed inversion method, we analyze the experimental data obtained from a high-frequency inductor when measuring the tangential magnetic field distribution at a close distance. The inductor (Fig. 7) is a 60 turn copper wire wound on a ferromagnetic core of relative permeability 1200.

The results shown in Fig. 8 illustrate variations of the measured tangential magnetic field at frequency f = 48 MHz on the near-field plane (h_1 = 10 mm). Using the measured data, the equivalent current distribution on the PCB is reconstructed, as shown in Fig. 9. To examine the accuracy of the proposed method for computing the equivalent current, we compute the the predicted tangential magnetic field on a far-field plane (h_2 = 50 mm). A comparison of the results shown in Fig. 10 with those obtained experimentally confirms the validy of the proposed method.

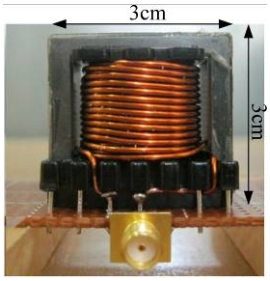

Fig. 7. High frequency inductor.

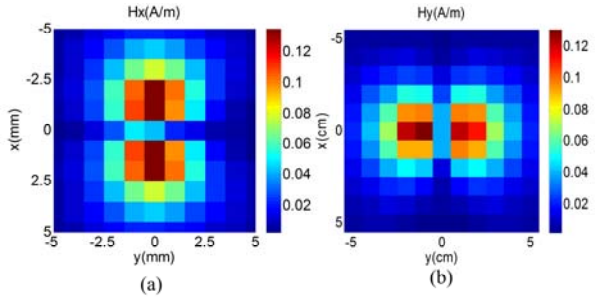

Fig. 8. Variations of the measured tangential magnetic field produced by the high frequency inductor on the near-field plane (h_1 =10 mm); (a) H_x and (b) H_y.

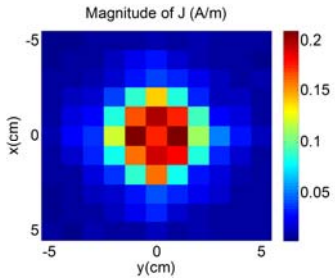

Fig. 9. Variations of the equivalent current ($|J|$) on the PCB plane (z = 0) predicted by the proposed model, using the data shown in Fig. 8.

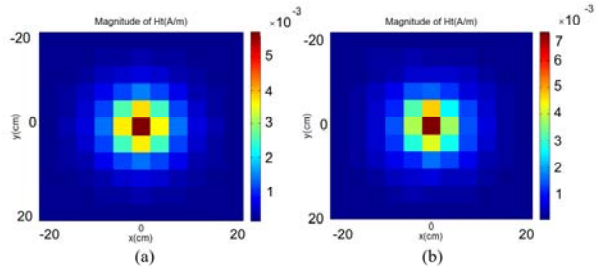

Fig. 10. Variations of the tangential magnetic field ($\sqrt{H_x^2+H_y^2}$) produced by high frequency inductor on the far-field plane (h_2 = 50 mm); (a) reconstructed and (b) measured results.

C. Microstrip transmission line

Another case used for validation of the proposed method, is microstrip transmission line. Figure 11 shows the structure of the microstrip transmission line. Microstrip fed by a sinusoidal source and terminated with a 50 Ω load. The results shown in Fig. 12 illustrate variations of the measured tangential magnetic field at frequency f = 30 MHz on the near-field plane (h_1 = 10 mm). Using the measured data, the equivalent current distribution on the PCB is reconstructed, as shown in Fig. 13. Using calculated equivalent current, we compute the predicted tangential magnetic field on a far-field plane (h_2 = 50 mm). A comparison of the results shown in Fig. 14 with those obtained experimentally confirms the validity of the proposed method.

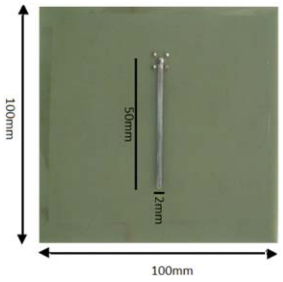

Fig. 11. Microstrip transmission line.

VI. CONCLUSION

In this paper we proposed a modeling technique, based on the electromagnetic equivalence principle, for prediction of radiated magnetic field from switch-mode power supply components. In this approach we substitute the radiating source by equivalent currents that

produce same field as original radiating source. These equivalent currents are calculated based on near field measurements. It is shown that the proposed model is readily converged for a wide range of sampling distances on the field measurement plane. However, the number of measurement data should be large enough to achieve accurate results. Theoretical results supported by experiments have confirmed the accuracy of the proposed technique.

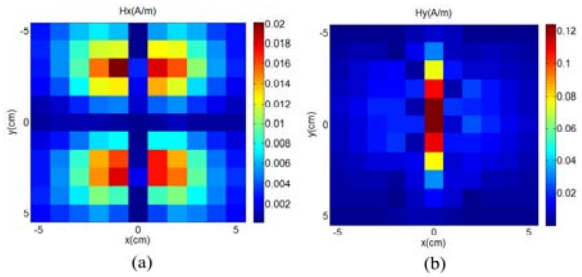

Fig. 12. Variations of the measured tangential magnetic field produced by the microstrip transmission line on the near-field plane (h_1 = 10 mm); (a) H_x and (b) H_y.

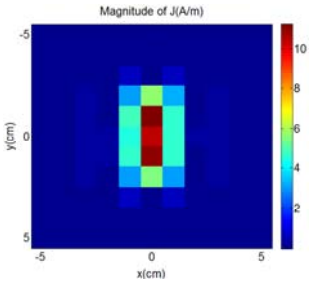

Fig. 13. Variations of the equivalent current ($|J|$) on the PCB plane (z = 0) predicted by the proposed model, using the data shown in Fig. 12.

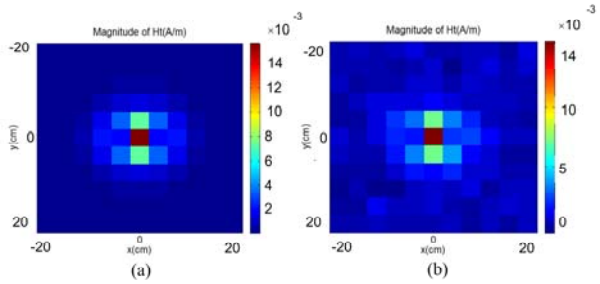

Fig.14. Variations of the tangential magnetic field ($\sqrt{H_x^2+H_y^2}$) produced by micro strip transmission line on the far-field plane (h_2=50mm); (a) reconstructed and (b) measured results.

REFERENCES

[1] G. Antonini, S. Cristina, and A. Orlandi, "EMC characterization of SMPS device circuit and radiated emission model," *IEEE Trans. Electromagn. Compat.*, vol. 38, no. 3, pp. 300-309, 1996.

[2] A. M. Sitzia, A. E. Baker, T. W. Preston, A. Puzo, and A. Pons, "Finite element analysis for power electronics EMC applications," *IEEE Trans. Magn.*, vol. 32, no. 3, pp. 1517-1520, 1996.

[3] N. J. Ryan, B. Chambers, and D. A. Stone, "FDTD modeling of heat sink RF characteristics for EMC mitigation," *IEEE Trans. Electromagn. Compat.*, vol. 44, no. 3, pp. 458-465, Aug. 2002.

[4] M. M. Hernando, A. Fernandez, M. Arias, M. Rodriguez, Y. Alvarez, and F. Las-Heras, "EMI radiated noise measurement system using the source reconstruction technique," *IEEE Trans. Ind. Electron.*, vol. 55, no. 9, pp. 3258-3265, 2008.

[5] L. Beghou, B. Liu, L. Pichon, and F. Costa, "Synthesis of equivalent 3-D models from near field measurements-application to the EMC of power printed circuit boards," *IEEE Trans. Magn.*, vol. 45, no. 3, pp. 1650-1653, Mar. 2009.

[6] M. Barzegaran and O. Mohammed, "Near field evaluation of electromagnetic signatures from wound rotor synchronous generators using wire modeling by finite elements," *28th Annual Review of Progress in Applied Computational Electromagnetics (ACES)*, pp. 774-779, Columbus, Ohio, April 2012.

[7] A. Nejadpak, M. R. Barzegaran, and O. A. Mohammed, "Evaluation of high frequency electromagnetic behavior of planar inductor designs for resonant circuits in switching power converters," *Applied Computational Electromagnetics Society (ACES) Journal*, vol. 26, no. 9, pp. 737-748, September 2011.

[8] K. Mainali and R. Oruganti, "Conducted EMI mitigation techniques for switch-mode power converters: A survey," *IEEE Trans. Power Electron.*, vol. 25, no. 9, pp. 2344 -2356, 2010.

[9] S. M. M. Mirtalaei, S. H. H. Sadeghi, and R. Moini, "Modeling the electric field emission of switch mode Power supplies using magnetic near-field measurement and method of moments," *Journal of Basic and Applied Science (JBASR)*, vol. 3, no. 2, pp. 597-602, February 2013.

[10] S. M. M. Mirtalaei, S. H. H. Sadeghi, and R. Moini, "Radiated emission determination from near field measurements for EMI evaluation of switch mode power supplies components by method of moments," *Power Electronics, Drive Systems and Technologies Conference (PEDSTC)*, pp. 421-425, Tehran, Iran, February 2013.

[11] S. M. M. Mirtalaei, S. H. H. Sadeghi, and R. Moini, "A combined method-of-moments and near field measurements for EMI evaluation of switch-mode power supplies," *Accepted for Publication in IEEE Trans. Ind. Electron,* 2013.

[12] R. F. Harrington, *Time-Harmonic Electromagnetic Fields*, McGraw-Hill, New York, 1961.

[13] Y. A. Lopez, F. L. Andrs, M. R. Pino, and T. K. Sarkar, "An improved super-resolution source reconstruction method," *IEEE Trans. Instrum. and Meas.*, vol. 58, no. 11, pp. 3855-3866, 2009.

[14] A. Balanis, *Antenna Theory: Analysis and Design*, John Wiley & Sons, 2005.

[15] Roger F. Harrington, *Field Computation by Moment Methods*, Macmillan, 1968.

[16] C. Paige and M. A. Saunders, "LSQR: An algorithm for sparse linear equations and sparse least squares," *ACM Trans. Math. Soft.*, vol. 8, pp. 43-71, 1981.

[17] K. Srinivasan, H. Sasaki, M. Swaminathan, and R. Tummala , "Calibration of near field measurements using microstrip line for noise predictions," *Proceedings of 54th Electronic Components and Technology Conference,* 2004.

Sayyed Mohammad Mehdi Mirtalaei received the B.Sc. degree in Electrical Engineering from Isfahan University of Technology (IUT), Isfahan, Iran, in 2005. He received the M.Sc. and Ph.D. degrees in Electrical Engineering from Amirkabir University of Technology (AUT), Tehran, Iran, in 2007 and 2013, respectively. Dr. Mirtalaei is Assistant Professor of Electrical Engineering at Islamic Azad University – Najafabad Branch, Isfahan, Iran. His research interest is power electronics, EMI/EMC and numerical method in electromagnetics.

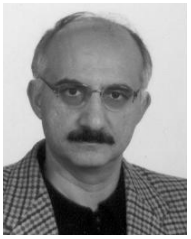

Seyed Hossein H. Sadeghi received the B.Sc. degree in Electrical Engineering from Sharif University of Technology, Tehran, Iran, the M.Sc. degree in Power Engineering from the University of Manchester Institute of Science and Technology, Manchester, England, and the Ph.D. degree in Electronic Systems Engineering from Essex University, Colchester, U.K., in 1980, 1984, and 1991, respectively.

In 1992, he was appointed as a Research Assistant Professor at Vanderbilt University, Nashville, TN. During 1996-1997, and 2005-2006 he was a Visiting Professor at the University of Wisconsin, Milwaukee. Dr. Sadeghi is a Professor of Electrical Engineering at Amirkabir University of Technology, Tehran, Iran. He holds 3 patents and is the author or coauthor of one book and over 250 scientific papers published in reviewed journals and presented at international conferences. His current research interests include electromagnetic non-destructive evaluation of materials and electromagnetic compatibility issues in power engineering. He is currently a visiting professor with the University of Wisconsin, Milwaukee.

Rouzbeh Moini received the B.Sc., M.Sc., and Ph.D. degrees in Electronics from Limoges University, Limoges, France in 1984, 1985, and 1988, respectively. In 1988, he joined the department of Electrical Engineering, Amirkabir University of Technology, Tehran, Iran. From 1995 to 1996, he was a visiting Professor with the University of Florida, Gainesville. Dr. Moini is a professor of Electrical Engineering with Amirkabir University of Technology. He is the author or coauthor of more than 200 scientific publications in reviewed journals and international conferences. His current research interests include numerical methods in electromagnetics, electromagnetic compatibility, and antenna theory. He is currently a visiting Professor with the University of Toronto, Canada.